Research Article

Nonlinear Elasticity of Borocarbide Superconductor YNi$_2$B$_2$C: A First-Principles Study

Lili Liu,[1,2] **Cai Chen,**[3] **Dingxing Liu,**[1] **Zhengquan Hu,**[1] **Gang Xu,**[1] **and Rui Wang**[2]

[1]*Department of Physics, Chongqing Three Gorges University, Chongqing 404100, China*
[2]*Institute for Structure and Function, Chongqing University, Chongqing 401331, China*
[3]*College of Civil Engineering, Chongqing Three Gorges University, Chongqing 404100, China*

Correspondence should be addressed to Lili Liu; liulili0612@163.com

First-principles calculations combined with homogeneous deformation methods are used to investigate the second- and third-order elastic constants of YNi$_2$B$_2$C with tetragonal structure. The predicted lattice constants and second-order elastic constants of YNi$_2$B$_2$C agree well with the available data. The effective second-order elastic constants are obtained from the second- and third-order elastic constants for YNi$_2$B$_2$C. Based on the effective second-order elastic constants, Pugh's modulus ratio, Poisson's ratio, and Vickers hardness of YNi$_2$B$_2$C under high pressure are further investigated. It is shown that the ductility of YNi$_2$B$_2$C increases with increasing pressure.

1. Introduction

Recently, a considerable number of superconducting binary, ternary, and quaternary Ni-based systems are reported [1] and Ni element is ferromagnetic; the identification of superconductivity in Ni-based compounds is of high current interest. Cava et al. [2] have synthesized the quaternary nickel borocarbides RNi$_2$B$_2$C (R=Y and rare earths) and found that Lu and Y compounds exhibit the highest superconducting transition temperatures (T_c = 16.6 and 15.6 K, resp.), while compounds with magnetic rare earths exhibit lower T_c: T_m (T_c = 11 K), E_r (T_c = 10.5 K), and H_o (T_c = 8 K). Because RNi$_2$B$_2$C [3] has the elevated superconducting transition temperature for some of the members of the family (R = Lu, Y) or the interesting interaction between superconductivity and magnetic ordering phenomena for the compounds with R = magnetic rare earth, considerable theoretical as well as experimental attention has been focused on these quaternary Ni-based compounds. Early work reported that single crystal YNi$_2$B$_2$C, one of the quaternary intermetallic compounds, is a traditional and isotropic superconductor. Therefore, a lot of work including theory and experiment has been done to examine various properties of YNi$_2$B$_2$C [4–10]. For example, Godart el al. [11] systematically investigated the structural, superconducting, and magnetic properties of YNi$_2$B$_2$C by X-ray diffraction measurements. Lee et al. [12] systematically researched the electronic structures of Ni-based superconducting quaternary compounds YNi$_2$B$_2$X (X = B, C, N, and O) by employing the linearized muffin-tin orbital band method. Meenakshi et al. [13] investigated the high pressure behavior of YNi$_2$B$_2$C at room temperature by electrical resistivity, thermopower, and X-ray diffraction incorporating imaging plate. More recently, Wang et al. [3] calculated the elastic and electronic structure properties of YNi$_2$B$_2$C under pressure by performing the generalized gradient approximation (GGA) and local density approximation (LDA) correction scheme in the frame of density functional theory (DFT). All these researches are very important to the further scientific and technical investigations.

At it is well known, elastic constants of a solid are important since some physical properties such as the bulk modulus, shear modulus, Young's modulus, and Poisson's ratio can be derived from the elastic constants and the strength of materials and the velocity of sound of longitudinal wave and shear wave can be also determined from its elastic constants [14]. In the finite-strain theory of elastic deformation, the second-order elastic constants (SOECs) are sufficient to describe the linear elastic stress-strain response [15]. In nonlinear elastic

theory, high-order elastic constants, such as third-order elastic constants (TOECs), play an important role as well as SOECs [16]. TOECs not only are useful in describing the mechanical response of crystals under high stress and strain, but also serve as a basis for describing anharmonic properties such as thermal expansion, phonon-phonon interaction, and Grüneisen parameter [17, 18]. Though many experiments have been performed to determine SOECs and high-order elastic constants [19], to obtain a complete set of TOECs is still important. However, the TOECs are very difficult to measure experimentally. Recently, a simple method using first-principles calculations has been employed to determine TOECs [20–22], and their results show good agreement with experiments. So far, as we know, the nonlinear elasticity as well as TOECs in YNi_2B_2C has not been reported in the literature. To understand the physical properties of YNi_2B_2C and provide significant information with respect to applications of YNi_2B_2C, it is very necessary to study the nonlinear elastic properties. In this paper, the complete set of TOECs for YNi_2B_2C are presented from first-principles calculations combined with the method of homogeneous deformation, and the effective SOECs are also obtained.

2. Theory and Computational Details

Our method for calculating elastic constants mentions homogeneous continuum elasticity theory [23–25]. After applying a finite homogeneous deformation to a material, the initial configuration x_i at the equilibrium will move to the final configuration x_i'. The deformation gradient is described as follows:

$$F_{ij} = \frac{\partial x_i'}{\partial x_j}. \tag{1}$$

From the deformation gradients, we may define the Lagrangian strain

$$\eta_{ij} = \frac{1}{2} \sum_{p=1}^{3} \left(F_{pi} F_{pj} - \delta_{ij} \right). \tag{2}$$

The elastic energy (ΔE) can be expanded in a Taylor series in terms of the strain tensor:

$$\Delta E = \frac{V}{2!} \sum_{ijkl} C_{ijkl} \eta_{ij} \eta_{kl} + \frac{V}{3!} \sum_{ijklmn} C_{ijklmn} \eta_{ij} \eta_{kl} \eta_{mn}, \tag{3}$$

where V is the volume of the unstrained lattice. When the elastic energy ΔE is the internal energy U and the Helmholtz free energy F, the elastic constants represent the isentropic and isothermal, respectively. Since our first-principles calculations are performed at 0 K, $F = U - TS = U$, the isentropic elastic constants are equal to the isothermal elastic constants. After using the Voigt notation for the strain tensors $\eta_{11} \rightarrow \eta_1$, $\eta_{22} \rightarrow \eta_2$, $\eta_{33} \rightarrow \eta_3$, $\eta_{23} \rightarrow \eta_4/2$, $\eta_{31} \rightarrow \eta_5/2$, and $\eta_{12} \rightarrow \eta_6/2$, (3) can be simply expressed as

$$\Delta E = \frac{V}{2!} \sum_{i,j=1}^{6} C_{ij} \eta_i \eta_j + \frac{V}{3!} \sum_{i,j,k=1}^{6} C_{ijk} \eta_i \eta_j \eta_k. \tag{4}$$

For YNi_2B_2C with tetragonal structure, there are six independent SOECs and twelve independent TOECs. The number of applied strain tensors must be as large as the number of independent TOECs for solving the TOECs. To obtain all the SOECs and TOECs of YNi_2B_2C, we select twelve simple deformation modes such that the strain tensor only has one or a few components. Any nonzero component of each strain tensor is denoted by a single scalar parameter ξ. After inserting various strain tensors into the above strain energy, we can find that the strain energy can be expressed as a polynomial function of the strain tensor parameter ξ; namely,

$$\Phi = \frac{\Delta E}{V} = \frac{1}{2}\Lambda_2 \xi^2 + \frac{1}{6}\Lambda_3 \xi^3 + O\left(\xi^4\right), \tag{5}$$

where the coefficients Λ_2 and Λ_3 are of SOECs and TOECs of the crystals, respectively. The selected twelve strain tensors A_α ($\alpha = 1, 2, \ldots, 12$) and the corresponding coefficients Λ_2 and Λ_3 are presented in Table 1. For each strain tensor A_α, the strain parameter ξ varies from -0.05 to 0.05 with a finite step size 0.005.

We have performed first-principles calculations based on the DFT level, using the VASP code developed at the Institut für Materialphysik of Universität Wien [26–28]. The ultrasoft pseudopotentials are employed to describe the electron-ion interactions. To compare the performance of different approximations of exchange-correlation interaction, in the structure calculations of YNi_2B_2C, both the GGA proposed by Perdew and Wang [29] and the LDA proposed by Vosko et al. [30] are considered as the exchange-correlation potential. For the elastic constants calculation, the effects of exchange-correlation interaction are treated with the GGA. For the Brillouin zone (BZ) integrals, reciprocal space is represent by the Monkhorst-Pack special k-point scheme [31]. Since high accuracy is needed to calculate the TOECs, the k-point mesh size with $15 \times 15 \times 5$ and cutoff energy with 550 eV are used to calculate the lattice and elastic constants. The total-energy of electronic self-consistency is converged to 10^{-6} eV. All the calculations avoid wrap-around errors and use an augmentation grid that is exactly twice as large as the coarse grid for the representation of the pseudo wave functions.

3. Results and Discussion

3.1. Structure Parameters. For the tetragonal structure YNi_2B_2C, the initial structural model is built according to previous available lattice parameters a and c. The tetragonal YNi_2B_2C has $I4/mmm$ space group and its crystal structure is shown in Figure 1. In a unit cell, the atom of Y is set at position $(0, 0, 0)$, the two Ni atoms are set at positions $(0, 0.5, 0.25)$ and $(0, 0.5, 0.75)$, the two B atoms are set at positions $(0, 0, z)$ and $(1, 1, 1 - z)$, and the C atom is set at position $(0, 0, 0.5)$. We optimize the structural parameters; full relaxations are carried out with respect to the volume, shape, and all internal atomic positions for the unit cell. In Table 2, we list our results together with the available experimental data [10, 11, 32, 33] and other theoretical results [1, 3]. The optimized lattice parameters are $a = 3.543$ Å, $c = 10.428$ Å from the GGA method and $a = 3.478$ Å, $c = 10.188$ Å from

TABLE 1: Selected strain tensors and the coefficients Λ_2 and Λ_3 in equation (5) as the linear combinations of the second- and third-order elastic constants for tetragonal crystal.

Strain	Λ_2	Λ_3
$A_1 = (\xi, 0, 0, 0, 0, 0)$	C_{11}	C_{111}
$A_2 = (\xi, \xi, 0, 0, 0, 0)$	$2C_{11} + 2C_{12}$	$2C_{111} + 6C_{112}$
$A_3 = (0, 0, \xi, 0, 0, 0)$	C_{33}	C_{333}
$A_4 = (\xi, 0, \xi, 0, 0, 0)$	$C_{11} + 2C_{13} + C_{33}$	$C_{111} + 3C_{113} + 3C_{133} + C_{333}$
$A_5 = (\xi, 0, -\xi, 0, 0, 0)$	$C_{11} - 2C_{13} + C_{33}$	$C_{111} - 3C_{113} + 3C_{133} - C_{333}$
$A_6 = (\xi, \xi, \xi, 0, 0, 0)$	$2C_{11} + 2C_{12} + 4C_{13} + C_{33}$	$2C_{111} + 6C_{112} + 6C_{113} + 6C_{123} + 6C_{133} + C_{333}$
$A_7 = (\xi, 0, 0, 2\xi, 0, 0)$	$C_{11} + 4C_{44}$	$C_{111} + 12C_{144}$
$A_8 = (\xi, 0, 0, 0, 2\xi, 0)$	$C_{11} + 4C_{44}$	$C_{111} + 12C_{155}$
$A_9 = (\xi, 0, 0, 0, 0, 2\xi)$	$C_{11} + 4C_{66}$	$C_{111} + 12C_{166}$
$A_{10} = (0, 0, \xi, 2\xi, 0, 0)$	$C_{33} + 4C_{44}$	$C_{333} + 12C_{344}$
$A_{11} = (0, 0, \xi, 0, 0, 2\xi)$	$C_{33} + 4C_{66}$	$C_{333} + 12C_{366}$
$A_{12} = (0, 0, 0, 2\xi, 2\xi, 2\xi)$	$8C_{44} + 4C_{66}$	$48C_{456}$
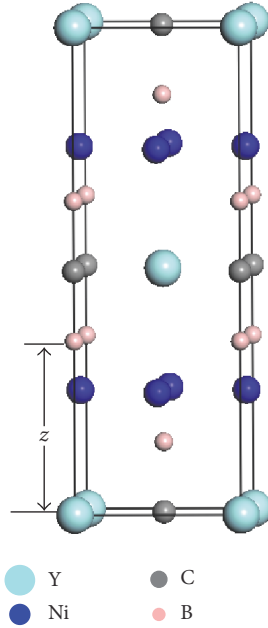
FIGURE 1: Crystal structure of YNi_2B_2C.

the LDA method. The results with GGA are slightly larger than those with LDA. Comparing with the results with LDA, the results with GGA are closer to the previous results. We also obtained the crystal coordinate $z = 0.358$ from the GGA method, which agrees well with the results by Wang et al. [3], Ravindran et al. [1], and Siegrist et al. [32] but is far from that by Belger et al. [33]. The crystal coordinate obtained from the LDA method is 0.355; the difference between GGA and LDA is small; however, the result from GGA is closer to the experimental results. In a word, from the structural parameters, it is found that the results from GGA seem to be the best. Therefore, in the following, the calculations with GGA are used to obtain the SOECs and TOECs of YNi_2B_2C.

3.2. The SOECs and TOECs.

The strain-energies for YNi_2B_2C, including the results of the first-principles calculations and the fitted polynomials, are shown in Figure 2. The discrete points denote the values from the first-principles calculations and the solid lines represent the results determined from the third-order polynomial fitting. It is worth noting that for YNi_2B_2C with Lagrangian strains up to 5.0%, including the terms up to third order in energy expansion sufficed to obtain good agreement with our ab initio results. In other words, the terms up to the third order in energy expansion produce the reliable results. Furthermore, we focus on examining for which range of strains the third-order effects dominate the properties of YNi_2B_2C. Taking A_6 as an example, Figure 3 shows the curves of the linear elasticity in comparison with nonlinear elasticity as well as the first-principles calculations. It is easily found that the linear elasticity is not sufficient and the relative error between the linear elasticity and the nonlinear elasticity is larger than 11.3% in strain energy density when the applied strain is larger than about 3.0%, so the nonlinear elasticity needs to be considered.

Knowledge of the values of elastic constants is crucial for understanding the structural stability, the bonding characteristic between the adjacent atomic planes, and the anisotropic character of the bonding. Table 3 gives the present SOECs as well as the experimental results [7, 8] and the other theoretical data [3]. For SOECs values, sometimes we possibly obtain slightly different results from different fitted curves. For example, C_{13} calculated from coefficients in $A_4(\xi)$, $A_5(\xi)$, and $A_6(\xi)$ are 136.74 GPa, 132.84 GPa, and 137.47 GPa, respectively, and C_{44} calculated from coefficients in $A_7(\xi)$, $A_8(\xi)$, and $A_{10}(\xi)$ are 62.60 GPa, 65.07 GPa, and 59.32 GPa, respectively. In these cases, we give the average of all obtained values in Table 3. It is found that our values of SOECs provide good agreement with the results obtained from the previous calculations and experiments, which provides guarantee for calculating the TOECs accurately. Obviously, the calculated elastic constants of YNi_2B_2C obey

TABLE 2: Calculated lattice parameters at $T = 0$ K and $P = 0$ GPa compared with the experimental data and other theoretical results.

Ref. number	Methods	a/Å	c/Å	c/a	z
Present	VASP ultrasoft GGA	3.543	10.428	2.943	0.358
	VASP ultrasoft LDA	3.478	10.188	2.929	0.355
[1]	LMTO	3.507	10.485	2.937	0.353
	CASTEP ultrasoft GGA	3.597	10.433	2.9	0.358
	CASTEP ultrasoft LDA	3.477	10.232	2.943	
[3]	CASTEP OTF GGA	3.541	10.482	2.960	
	CASTEP OTF LDA	3.479	10.256	2.948	
	CASTEP norm-conserving GGA	3.667	10.947	2.985	
	CASTEP norm-conserving LDA	3.726	10.617	2.849	
[10]	Exp. (neutron scattering)	3.51	10.53	3.0	
[11]	Exp. (X-ray diffraction, 300 K)	3.524	10.545	2.992	0.375
[32]	Exp. (X-ray reflections)	3.526	10.543	2.990	0.358
[33]	Exp. (single crystal diffraction)	3.5258	10.5425	2.990	0.1409
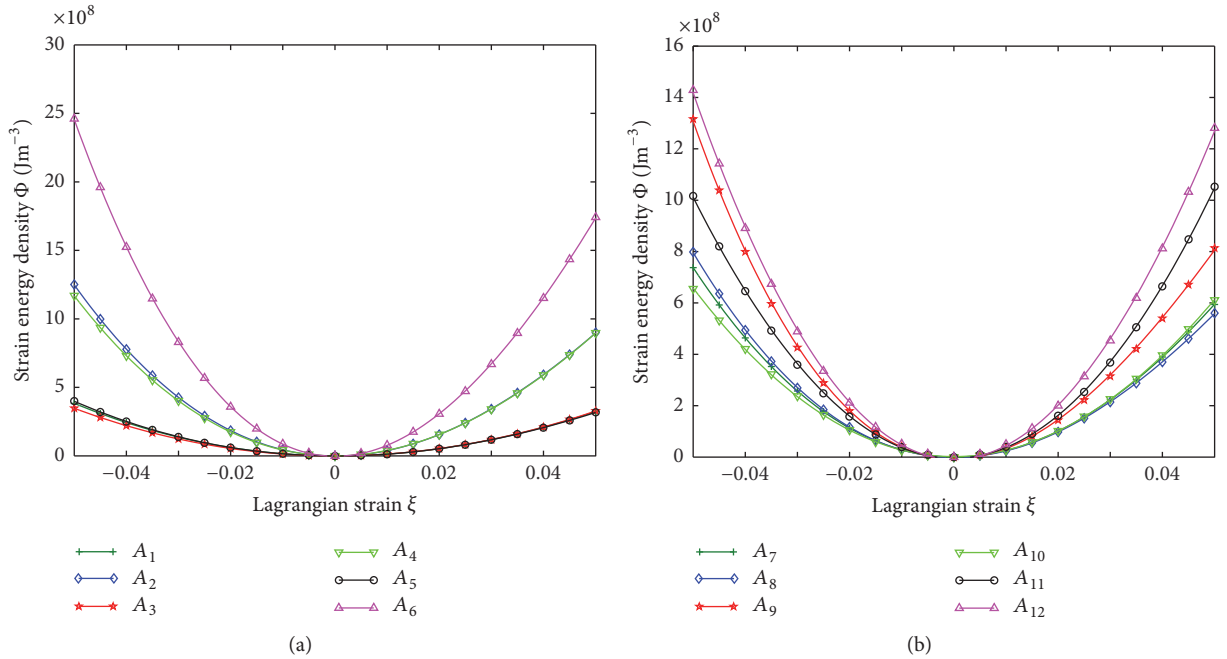
FIGURE 2: The strain energy relations for tetragonal YNi_2B_2C. The discrete points denote the values from first-principles calculations and the solid curves represent the results obtained from the third-order polynomial fitting.

the following well-known mechanical stability criteria [34] for the tetragonal structure:

$$C_{11} > |C_{12}|,$$
$$2C_{13}^2 < C_{33}(C_{11} + C_{12}),$$
$$C_{44} > 0,$$
$$C_{66} > 0.$$

(6)

Thus, YNi_2B_2C with tetragonal structure is mechanically stable at the ground state. The elastic constants C_{11} and C_{33} are directly related to sound propagation along the crystallographic direction, while other shear elastic constants

(C_{12}, C_{13}, C_{44}, and C_{66}) are dominated along the nonaxial sound propagation. The results show that it has larger C_{ij} along the axial directions rather than the nonaxial directions indicating that it is more uncompressible along axial directions. We care, moreover, that $C_{11} > C_{33}$, which indicates that the atomic bonding strength along the [100] direction between the nearest neighbors is stronger than that along the [001] direction.

The calculated TOEC values of tetragonal YNi_2B_2C single crystal are summarized in Table 4. Unfortunately, there are currently no experimental and other theoretical values for comparison. It is known that the TOECs provide a comprehensive knowledge concerning the vibrational anharmonicity of the acoustic modes in long-wavelength limit. From Table 4,

TABLE 3: Second-order elastic constants C_{ij} (GPa) of tetragonal YNi_2B_2C at 0 K and 0 GPa, in comparison with the previous calculations and available experimental measurements.

Ref. number	Methods	C_{11}	C_{12}	C_{13}	C_{33}	C_{44}	C_{66}
Present	VASP ultrasoft GGA	282.60	147.22	135.68	269.91	62.33	140.68
[3]	CASTEP GGA and OTF	292.7	133.6	138.6	282.4	68.6	129.8
	Exp. (RUS, 300 K)	294.6	157.7	125.6	261.5	64.4	142.1
[7]	Exp. (time-of-flight, 300 K)	284.7	145.7	—	—	67.1	143.3
	Exp. (time-of-flight, 2 K)	292	149.8	—	—	67.4	132
[8]	Exp. (time-of-flight, 14.2 K)	222	102[a]	—	212	54.5	131

[a]Calculated from the quoted values of C_{11} and $(C_{11} - C_{12})/2$ [8].

TABLE 4: Third-order elastic constants (C_{ijk}) of tetragonal YNi_2B_2C (in GPa).

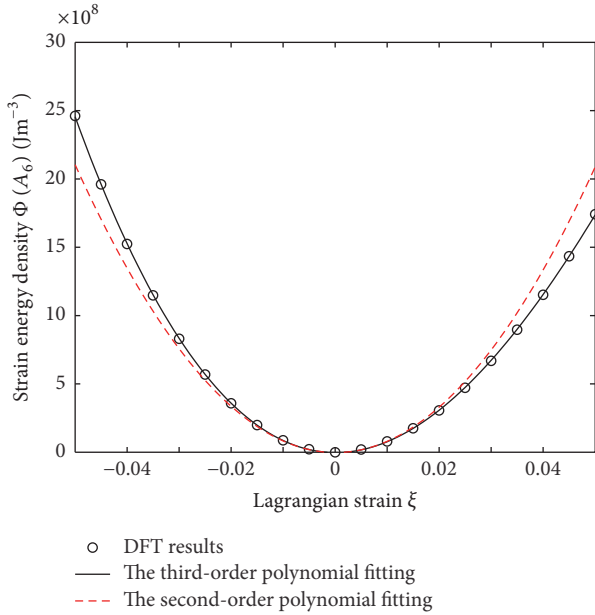| C_{111}	C_{112}	C_{113}	C_{123}	C_{133}	C_{144}	C_{155}	C_{166}	C_{333}	C_{344}	C_{366}	C_{456}
−1136.50	−945.04	−624.38	195.47	−973.51	−173.89	−358.18	−889.92	−494.51	−43.66	111.09	−70.61

FIGURE 3: Energy as a function of the Lagrangian strain parameter ξ for the particular strain tensor A_6. The circles indicate the values of the first-principles calculations; solid and dashed curves represent the results obtained from nonlinear and linear elasticity theory, respectively.

it is observed that the TOECs values of tetragonal YNi_2B_2C are calculated to be negative except for two positive values of C_{123} (=195.47 GPa) and C_{366} (=111.09 GPa). Furthermore, the absolute value of C_{111} is the greatest among the TOECs indicating the anisotropy along the basal plane to be more pronounced than along the unique axis.

3.3. Elastic Properties under Pressure. It is helpful to describe the effective SOECs under different pressure using the SOECs and TOECs. The effective SOECs C_{ij}^P of a crystal can be obtained when subjected to pressure P. For YNi_2B_2C with tetragonal structure, the expressions for the six effective SOECs are as follows [35]:

$$C_{11}^P = C_{11} + \eta \left(4C_{11} + 2C_{12} + C_{111} + C_{112}\right)$$
$$+ \zeta \left(-C_{11} + 2C_{13} + C_{113}\right),$$

$$C_{12}^P = C_{12} + \eta \left(2C_{12} + 2C_{112}\right) + \zeta \left(-C_{12} + 2C_{123}\right),$$

$$C_{13}^P = C_{13} + \eta \left(C_{113} + C_{123}\right) + \zeta \left(C_{13} + C_{133}\right),$$

$$C_{33}^P = C_{33} + \eta \left(4C_{13} - 2C_{33} + 2C_{133}\right)$$
$$+ \zeta \left(5C_{33} + C_{333}\right), \tag{7}$$

$$C_{44}^P = C_{44} + \eta \left(\frac{1}{2}C_{11} + \frac{1}{2}C_{12} + C_{13} + C_{144} + C_{155}\right)$$
$$+ \zeta \left(\frac{1}{2}C_{13} + \frac{1}{2}C_{33} + C_{44} + C_{344}\right),$$

$$C_{66}^P = C_{66} + \eta \left(C_{11} + C_{12} + 2C_{66} + 2C_{166}\right)$$
$$+ \zeta \left(C_{13} - C_{66} + C_{366}\right),$$

where the Lagrangian strains η and ζ can be obtained in terms of the pressure P and SOECs as

$$\eta = \frac{(C_{13} - C_{33})P}{(C_{11} + C_{12})C_{33} - C_{33}^2},$$

$$\zeta = \frac{2(C_{13} - C_{11} - C_{12})P}{(C_{11} + C_{12})C_{33} - C_{33}^2}. \tag{8}$$

The variation of the effective SOECs C_{ij}^P with pressure in the range of 0–5 GPa for YNi_2B_2C on the basis of the calculated SOECs and TOECs is shown in Figure 4. It is observed that the longitudinal mode C_{11} as well as the shear modes C_{12}, C_{13}, C_{44}, and C_{66} of YNi_2B_2C can increase linearly; in contrast the longitudinal mode C_{33} decreases linearly
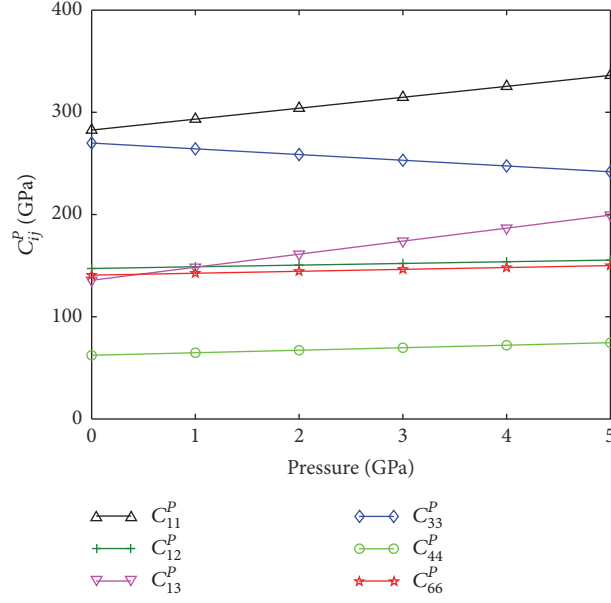
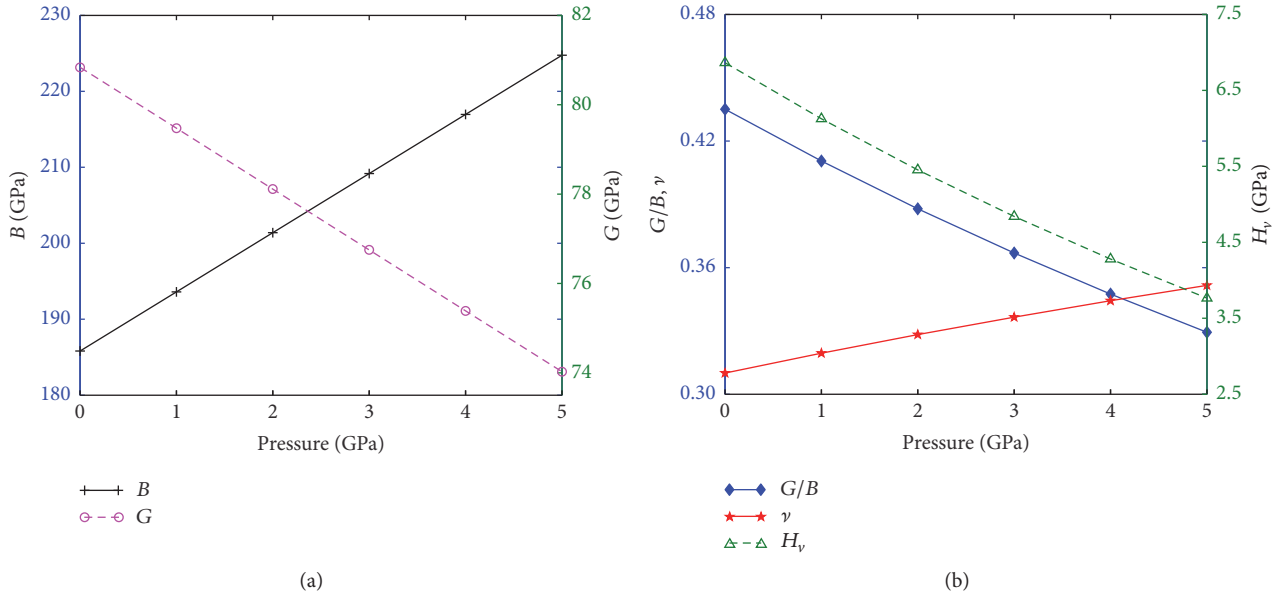FIGURE 4: The effective second-order elastic constants (C_{ij}^P) versus pressure (P) of tetragonal YNi$_2$B$_2$C.

(a)

(b)

FIGURE 5: The pressure dependence of (a) B and G and (b) G/B, ν, and H_ν.

with increasing the pressure. C_{11} and C_{13} move up very sharply, and C_{12}, C_{44}, and C_{66} have the same growth rate. For a tetragonal crystal, the mechanical stability leads to restrictions on the elastic constants under pressure as follows [36]: $\widetilde{C}_{11}^P - \widetilde{C}_{12}^P > 0$, $\widetilde{C}_{11}^P + \widetilde{C}_{33}^P - 2\widetilde{C}_{13}^P > 0$, $\widetilde{C}_{ii}^P > 0$, and $2\widetilde{C}_{11}^P + \widetilde{C}_{33}^P + 2\widetilde{C}_{12}^P + 4\widetilde{C}_{13}^P > 0$, where $\widetilde{C}_{\alpha\alpha}^P = C_{\alpha\alpha}^P - P$ ($\alpha = 1, 3, 4, 6$), $\widetilde{C}_{12}^P = C_{12}^P + P$, and $\widetilde{C}_{13}^P = C_{13}^P + P$. It is obvious that the elastic constants of YNi$_2$B$_2$C satisfy all of these conditions in the pressure range of 0–5 GPa.

The bulk modulus B represents the resistance of a material to volume (bond-length) change under hydrostatic pressure, and the shear modulus G describes the resistance to shape

(angle-bond) change caused by a shearing force. Materials with high bulk modulus but low shear modulus will reflect good ductility. The bulk modulus B and shear modulus G can be calculated by $B = (1/9)(2C_{11}^P + 2C_{12}^P + 4C_{13}^P + C_{33}^P)$ and $G = (1/15)(2C_{11}^P - C_{12}^P - 2C_{13}^P + C_{33}^P + 6C_{44}^P + 3C_{66}^P)$ [37]. Substituting the values of the effective SOECs C_{ij}^P into the bulk modulus B and shear modulus G expressions, we can obtain the values of B and G under different pressure. Figure 5(a) shows the pressure dependence of B and G for YNi$_2$B$_2$C. It can be seen from Figure 5(a) that bulk modulus increases but the shear modulus reduces with increasing pressure, which indicates that the ductility of YNi$_2$B$_2$C increases with

increasing pressure. Based on the bulk modulus and the shear modulus, Pugh [38] has proposed that the quotient of G/B can predict the brittle and ductile behavior of materials, and thus a low value of G/B is associated with ductility while a high value is associated with brittleness. All the values of Pugh ratio G/B in the pressure range of 0–5 GPa are showed in Figure 5(b). Obviously, all the values of G/B decrease with pressure which means that pressure can improve ductility. In addition, Poisson's ratio with $\nu = (3B-2G)/2(3B+G)$ can also reflect the ductile properties. Poisson's ratio is reversely proportional to G/B [39]; that is to say, the larger the Poisson ratio, the better the ductility. Figure 5(b) also presents Poisson's ratio of YNi_2B_2C as a function of pressure. It is clearly shown that Poisson's ratio has the opposite change tendency with G/B; that is, we can obtain the same conclusion from the change of Poisson's ratio and G/B; namely, the ductility of YNi_2B_2C increases with increasing pressure. As we all known, both Pugh's modulus ratio and Poisson's ratio have close relationship with the hardness of materials. Hardness is another important parameter to describe the mechanical properties of a material. The formula of the Vickers hardness proposed by Chen et al. [40, 41] can be expressed as $H_v = 2(k^2G)^{0.585} - 3$, where $k = G/B$. The change in Vickers hardness versus pressure for YNi_2B_2C is shown in Figure 5(b). Obviously, the hardness of YNi_2B_2C decreases with increasing pressure. Besides, the low G/B ratio corresponds to poor hardness. Therefore, the ductility is enhanced with the decreasing of hardness.

4. Conclusions

In the present work, the SOECs and TOECs of tetragonal YNi_2B_2C are systematically investigated using first-principles methods combined with finite-strain theory. In comparison with the linear elastic theory, the nonlinear elastic effects must be considered when the applied strain is larger than about 3.0%. In terms of the SOECs and TOECs, the effective SOECs of YNi_2B_2C are presented. By the elastic stability criteria under isotropic pressure, it is predicted that YNi_2B_2C with tetragonal structure is mechanically stable in the pressure range of 0–5 GPa. Based on the effective SOECs, Pugh's modulus ratio, Poisson's ratio, and Vickers hardness of YNi_2B_2C under high pressure from 0 to 5 GPa are further investigated. Pugh's modulus ratio and the Vickers hardness decrease and Poisson's ratio increases with increasing pressure, resulting in a decrease of the hardness and an increase of the ductility of YNi_2B_2C.

Conflicts of Interest

The authors declare that they have no conflicts of interest.

Acknowledgments

References

[1] P. Ravindran, S. Sankaralingam, and R. Asokamani, "Electronic structure and phase-stability studies on superconducting YNi_2B_2C, YRh_3B, and nonsuperconducting YNi_4B," *Physical Review B*, vol. 52, no. 17, pp. 12921–12930, 1995.

[2] R. J. Cava, H. Takagi, H. W. Zandbergen et al., "Superconductivity in the quaternary intermetallic compounds $LnNi_2B_2C$," *Nature*, vol. 367, pp. 252-253, 1994.

[3] P. Wang, C.-G. Piao, R.-Y. Meng, Y. Cheng, and G.-F. Ji, "Elastic and electronic properties of YNi_2B_2C under pressure from first principles," *Physica B: Condensed Matter*, vol. 407, no. 2, pp. 227–231, 2012.

[4] R. Nagarajan, C. Mazumdar, Z. Hossain et al., "Bulk superconductivity at an elevated temperature ($T_c \approx 12$ K) in a nickel containing alloy system Y-Ni-B-C," *Physical Review Letters*, vol. 72, article 274, 1994.

[5] R. J. Cava, H. Takagi, B. Batlogg et al., "Superconductivity at 23 K in yttrium palladium boride carbide," *Nature*, vol. 367, no. 6459, pp. 146–148, 1994.

[6] R. J. Cava, H. Takagi, H. W. Zandbergen et al., "Superconductivity in the quaternary intermetallic compounds $LnNi_2B_2C$," *Nature*, vol. 367, pp. 252-253, 1994.

[7] P. M. C. Rourke, J. Paglione, F. Ronning, L. Taillefer, and K. Kadowaki, "Elastic tensor of YNi_2B_2C," *Physica C: Superconductivity and Its Applications*, vol. 397, no. 1-2, pp. 1–6, 2003.

[8] S. Isida, A. Matsushita, H. Takeya, and M. Suzuki, "Ultrasonic study on superconducting YNi_2B_2C," *Physica C: Superconductivity and Its Applications*, vol. 349, no. 1-2, pp. 150–154, 2001.

[9] G. H. Cao, P. Simon, W. Skrotzki, S. C. Wimbush, and B. Holzapfel, "TEM characterisation of YNi_2B_2C thin film microstructure," *Applied Physics A: Materials Science and Processing*, vol. 81, no. 3, pp. 583–585, 2005.

[10] L. Pintschovius, F. Weber, W. Reichardt et al., "Phonon linewidths in YNi_2B_2C," *Pramana*, vol. 71, no. 4, pp. 687–693, 2008.

[11] C. Godart, L. C. Gupta, R. Nagarajan et al., "Structural, superconducting, and magnetic properties of YNi2B2C and ErNi2B2C," *Physical Review B*, vol. 51, no. 1, pp. 489–496, 1995.

[12] J. I. Lee, T. S. Zhao, I. G. Kim, B. I. Min, and S. J. Youn, "Electronic structure of Ni-based superconducting quaternary compounds: YNi_2B_2X (X=B, C, N, and O)," *Physical Review B*, vol. 50, article 4030, 1994.

[13] S. Meenakshi, V. Vijayakumar, R. S. Rao et al., "High pressure study of borocarbide superconductor YNi_2B_2C at room temperature," *Physica B*, vol. 223-224, pp. 93–95, 1996.

[14] P. Ravindran, L. Fast, P. A. Korzhavyi, B. Johansson, J. Wills, and O. Eriksson, "Density functional theory for calculation of elastic properties of orthorhombic crystals: application to $TiSi_2$," *Journal of Applied Physics*, vol. 84, no. 9, pp. 4891–4904, 1998.

[15] M. Born and K. Huang, *DynaMical Theory of Crystal Lattices*, Oxford University Press, London, UK, 1956.

[16] R. N. Thurston and K. Brugger, "Third-order elastic constants and the velocity of small amplitude elastic waves in homogeneously stressed media," *Physical Review*, vol. 133, no. 6A, pp. A1604–A1610, 1964.

[17] Y. Hiki, "Higher Order Elastic Constants of Solids," *Annual Review of Materials Research*, vol. 11, pp. 51–73, 1981.

[18] X. D. Zhang, Z. Y. Jiang, B. Zhou, Z.-F. Hou, and Y.-Q. Hou, "High-order elastic constants and anharmonic properties of $NaBH_4$: first-principles calculations," *Chinese Physics Letters*, vol. 28, no. 7, Article ID 076201, 2011.

[19] R. Wang, S. Wang, X. Wu, and Y. Yao, "The third-order elastic moduli and pressure derivatives for AlRE (RE=Y, Pr, Nd, Tb, Dy, Ce) intermetallics with B2-structure: a first-principles study," *Solid State Communications*, vol. 151, no. 14-15, pp. 996–1000, 2011.

[20] M. Łopuszynski and J. A. Majewski, "Ab initio calculations of third-order elastic constants and related properties for selected semiconductors," *Physical Review B*, vol. 76, Article ID 045202, 2007.

[21] J. J. Zhao, J. M. Winey, and Y. M. Gupta, "First-principles calculations of second- and third-order elastic constants for single crystals of arbitrary symmetry," *Physical Review B*, vol. 75, Article ID 094105, 2007.

[22] H. Wang and M. Li, "Ab initio calculations of second-, third-, and fourth-order elastic constants for single crystals," *Physical Review B*, vol. 79, Article ID 224102, 2009.

[23] F. D. Murnaghan, *Finite Deformation of An Elastic Solid*, Chapman & Hall, London, UK, 1951.

[24] K. Brugger, "Thermodynamic definition of higher order elastic coefficients," *Physical Review*, vol. 133, no. 6A, pp. A1611–A1612, 1964.

[25] R. N. Thurston, *Physical Acoustics Principles and Methods*, Academic Press, New York, NY, USA, 1964.

[26] G. Kresse and J. Hafner, "Ab initio molecular dynamics for open-shell transition metals," *Physical Review B*, vol. 48, article 13115, 1993.

[27] G. Kresse and J. Furthmller, "Efficiency of ab-initio total energy calculations for metals and semiconductors using a plane-wave basis set," *Computational Materials Science*, vol. 6, no. 1, pp. 15–50, 1996.

[28] G. Kresse and J. Furthmller, "Efficient iterative schemes for ab initio total-energy calculations using a plane-wave basis set," *Physical Review B*, vol. 54, article 11169, 1996.

[29] J. P. Perdew and Y. Wang, "Accurate and simple analytic representation of the electron-gas correlation energy," *Physical Review B*, vol. 45, no. 23, pp. 13244–13249, 1992.

[30] S. H. Vosko, L. Wilk, and M. Nusair, "Accurate spin-dependent electron liquid correlation energies for local spin density calculations: a critical analysis," *Canadian Journal of Physics*, vol. 58, no. 8, pp. 1200–1211, 1980.

[31] H. J. Monkhorst and J. D. Pack, "Special points for Brillouin-zone integrations," *Physical Review. B. Solid State*, vol. 13, no. 12, pp. 5188–5192, 1976.

[32] T. Siegrist, H. W. Zandbergen, R. J. Cava, J. J. Krajewski, and W. F. Peck Jr., "The crystal structure of superconducting $LuNi_2B_2C$ and the related phase LuNiBC," *Nature*, vol. 367, no. 6460, pp. 254–256, 1994.

[33] A. Belger, U. Jaenicke-Rössler, D. Lipp, B. Wehner, P. Paufler, and G. Behr, "Structure refinement of the superconducting phase YNi_2B_2C as a function of temperature in the range 25–300 K," *Physica C: Superconductivity and Its Applications*, vol. 306, no. 3-4, pp. 277–288, 1998.

[34] F. Mouhat and F. X. Coudert, "Necessary and sufficient elastic stability conditions in various crystal systems," *Physical Review B*, vol. 90, Article ID 224104, 2014.

[35] R. R. Rao and A. Padmaja, "Effective second-order elastic constants of a strained crystal using the finite strain elasticity theory," *Journal of Applied Physics*, vol. 62, article 440, 1987.

[36] H. C. Zhai, X. F. Li, and J. Y. Du, "First-Principles Calculations on Elasticity and Anisotropy of Tetragonal Tungsten Dinitride under Pressure," *Materials Transactions*, vol. 53, pp. 1247–1251, 2012.

[37] W. Voigt, *Lehrbuch der Kristallphysik*, Teubner, Leipzig, Germany, 1928.

[38] S. F. Pugh, "Relations between the elastic moduli and the plastic properties of polycrystalline pure metals," *Philosophical Magazine*, vol. 45, pp. 823–843, 1954.

[39] H. Y. Niu, X. Q. Chen, P. T. Liu et al., "Extra-electron induced covalent strengthening and generalization of intrinsic ductile-to-brittle criterion," *Scientific Reports*, vol. 2, article 718, 2012.

[40] X.-Q. Chen, H. Niu, D. Li, and Y. Li, "Modeling hardness of polycrystalline materials and bulk metallic glasses," *Intermetallics*, vol. 19, no. 9, pp. 1275–1281, 2011.

[41] X. Q. Chen, H. Y. Niu, C. Franchini, D. Z. Li, and Y. Y. Li, "Hardness of *T*-carbon: Density functional theory calculations," *Physical Review B*, vol. 84, Article ID 121405, 2011.